

Corrosion Inhibition of 302 Stainless Steel with Schiff Base Compounds

S.M.A. Hosseini*, A. Azimi, I. Sheikhshoaei and M. Salari

Department of Chemistry, Faculty of Science, Shahid Bahonar University of Kerman, Kerman 76169, Iran

(Received 25 October 2008, Accepted 13 October 2009)

The effects of 2,2'-[bis-N(4-cholorobenzaldimin)]-1,1'-dithio (BCBD) and bis-(2-aminophenyl) disulphide (BAPD) on the corrosion behavior of 302 stainless steel in 0.5 M sulfuric acid solution as corrosive medium were investigated using weight loss and potentiostatic polarization techniques. Some corrosion parameters such as anodic and cathodic Tafel slopes, corrosion potential, corrosion current density, surface coverage degrees and inhibition efficiencies were calculated. The polarization measurements indicated that the inhibitors were of mixed type which inhibited corrosion by parallel adsorption on the surface of stainless steel due to the presence of more than one active centre in the inhibitor molecule. The adsorption followed Langmuir adsorption isotherm. The activation energy and thermodynamic parameters were calculated at different temperatures. Results showed that BCBD had a higher inhibition efficiency compared with BAPD.

Keywords: Corrosion, Sulfuric acid, Stainless steel 302, BCBD, BAPD (as an inhibitor)

INTRODUCTION

Stainless steel is a material frequently used for its properties of resistance to corrosion in both the industrial domain and the maritime field. Indeed, in contact with the air, the surface is quickly covered with a chromium and iron oxide layer, which increases the resistance to corrosion. The quality and the evolution of this protective film depend not only on the environmental conditions close to the metallic surface but also and mainly on the chromium content of the alloy.

Type 302 stainless steel (302SS) has found wide application in a wide variety of chemical industries. It is covered with a highly protective film of chromium oxyhydroxide and is also resistant to corrosion in many aggressive environments. Sulfuric acid solution, however, readily attacks 302SS. It is possible to reduce the corrosion rate to the safe level by adding some inhibitors. Most well-

known and investigated inhibitors for corrosion of steel in acidic solution are heterocyclic compounds [1-8]. For these inhibiting compounds, it is clear that the adsorption on the metal substrate is the initial step in inhibition. The adsorption inhibitor is related to the presence of heteroatoms such as nitrogen, oxygen, phosphorous and sulphur and carbon chain length as well as the triple bond or aromatic ring in their molecular structure. Generally, a stronger co-ordination bond causes higher inhibition efficiency (IE) [9]. Schiff bases condensation product of an amine and a ketone or aldehyde, and $R_2C=NR'$ as the general formula are known examples of this category, and have been investigated for the inhibition of acid corrosion of stainless steel [10-12], mild steel [13], aluminium [14] and copper [15]. An interesting phenomenon is that Schiff bases systematically display considerably stronger corrosion inhibition efficiencies than do the corresponding amines [10-11]. The explanation lies in the presence of unoccupied π^* -orbitals in the Schiff base molecule, which enable electron back-donation from the

*Corresponding author. E-mail: s.m.a.hosseini@mail.uk.ac.ir

transition metal d-orbitals and stabilize the existing metal-inhibitor bond, which is not possible with the amine [16]. The aim of the present work is to investigate the inhibitory effects of 2,2'-[bis-N(4-chloro-benzaldimin)]-1,1'-dithio (BCBD) and bis-(2-aminophenyl) disulphide (BAPD) on corrosion of stainless steel 302 in 0.5 M sulfuric acid.

EXPERIMENTAL

Material Preparation

Analytical reagent (AR) grade H_2SO_4 (MERCK) and double-distilled water were used for preparing test solutions of 0.5 M H_2SO_4 for all of the experiments. Schiff bases with structures shown in Fig. 1, the bidentate schiff BCBD, was synthesized by the reaction of 2, bis-(2-aminophenyl) disulphide with 4-cholorobenzaldehyde and BAPD was prepared according to the reaction presented in Fig. 1d. The product identity was confirmed *via* melting points, Fourier transform infrared (FT-IR) (Maston 1000 FT-IR) and proton nuclear magnetic resonance (^1H NMR) (Perkin Elmer C, H

and N Analyzer, model 2HOB). The compound was characterized through its spectral data and its purity was confirmed by thin-layer chromatography (TLC) and IR spectroscopy.

Electrodes

The 302 stainless steel composed of 0.15% C, 2% Mn, 0.045% P, 0.03% S, 17%-19% Cr, 8.00%-10% Ni and Fe balanced, was used in this investigation. The electrodes under investigation were abraded, and were polished successively by emery papers of different grades, *i.e.* 300-1200, cleaned in ultrasonic bath, and subsequently rinsed with double-distilled water and degreased with acetone and dried at room temperature. For polarization studies, metal was embedded in epoxy resin, to expose a geometrical surface area of 1 cm^2 to the electrolyte. Prior to these measurements, the exposed surface was pretreated in the same manner as for weight loss experiments. All experiments were carried out at a temperature of $20 \pm 1\text{ }^\circ\text{C}$, with the electrolyte solutions in equilibrium with the atmosphere (*i.e.* aerated solutions).

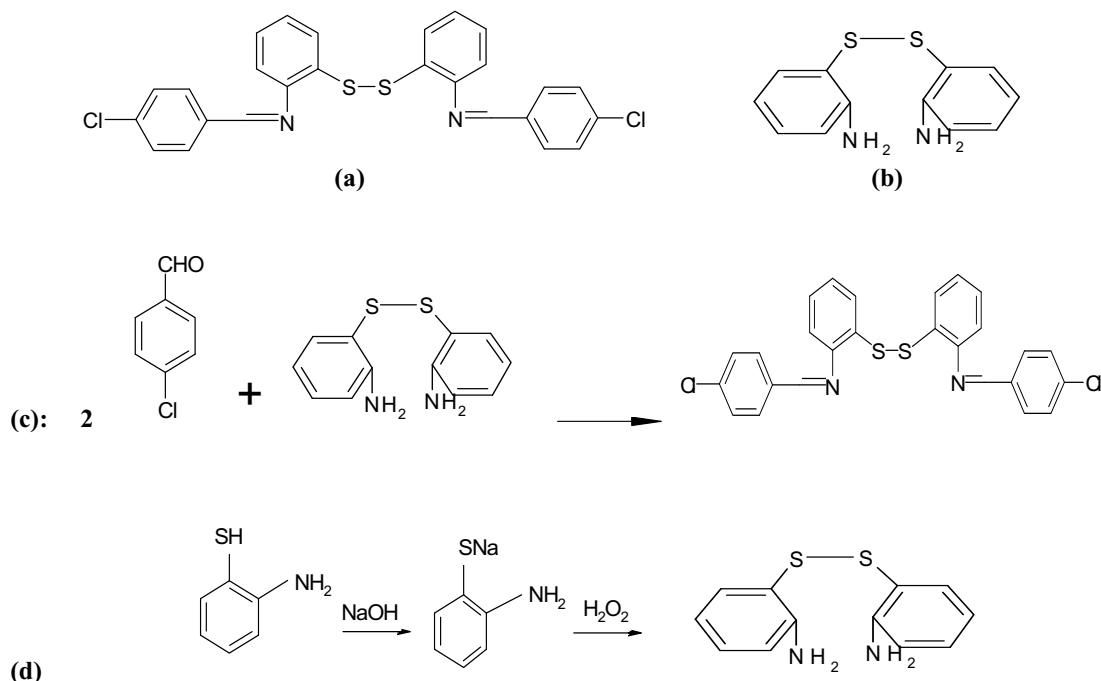


Fig. 1. Chemical structures of the investigated inhibitors: (a) BCBD (b) BAPD and synthesis methods of investigated inhibitors (c) BCBD (d) BAPD.

Weight Loss Measurements

The experiments were carried out in 0.5 M H₂SO₄ using cold rolled steel and as per ASTM, G31-71. The electrodes under investigation were abraded, and were polished successively by emery papers of different grades, *i.e.* 300-1200, cleaned in ultrasonic bath, and subsequently rinsed with double-distilled water and degreased with acetone and dried at room temperature. To be brief, stainless steel specimens in triplicate were immersed for a period of 24 h in 100 ml acid solution containing various concentrations of the inhibitors. The mass of the specimens before and after immersion was determined using an analytical balance accurate 0.1 mg. Relative differences between triplicate experiments were found to be smaller than 8%, indicating good reproducibility.

Electrochemical Studies

The electrochemical experiments were carried out in Pyrex cell with three compartments. A Pt foil auxiliary electrode was used as the counter electrode and a saturated calomel electrode (SCE) served as reference electrode.

Measurements were obtained using a potentiostat CG, CV& PG system model DPSWX (ZaG Chimi). Prior to the polarization measurements, the open-circuit potential became stable within 30 min, and after that all tests were performed at room temperature at constant sweep rate 2 mV s⁻¹. Inhibition efficiencies were determined from corrosion currents calculated by Tafel extrapolation method.

RESULTS AND DISCUSSION

Gravimetric Measurements

The corrosion rates of stainless steel in different concentrations of the inhibitors were calculated from expression (1):

$$W = \Delta m / At \quad (1)$$

where Δm is the loss in weight (mg), A is the area of the coupon (cm²) and t is the exposure time (h).

From the values of corrosion rate in the presence (W_{inh}) and absence (W_{blank}) of the inhibitors, their inhibition efficiencies (IE%) were respectively calculated from expression (2):

$$IE\% = [1 - w_{inh}/w_{blank}] \times 100 \quad (2)$$

Figures 2 and 3 show the variation of inhibition efficiency as a function of concentrations of inhibitors in 0.5 M H₂SO₄ at 20 ± 1 °C after 24 h of immersion. The results showed that inhibition efficiency increased as the concentration of the inhibitor rose from 4.1 M and 8 M to 16.2 × 10⁻⁵ M and 32 × 10⁻⁵ M of BCBD and BAPD, respectively. The increase of inhibitor efficiency with concentrations of inhibitors may be attributed to the formation of a barrier film which prevents attack of the metal surface by acid.

Polarization Measurements

Sulfuric acid (0.5 M) containing various concentrations of inhibitors (0, 20, 40 and 80 ppm) were used for potentiostatic

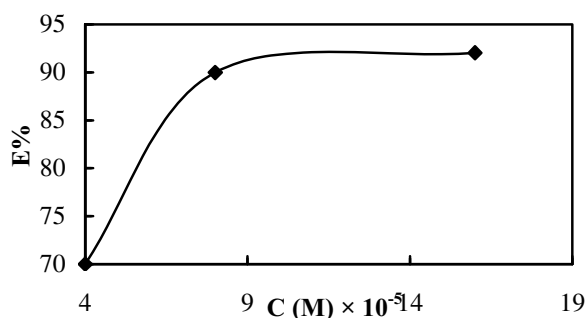


Fig. 2. Variation of the inhibition efficiency with different concentration of BCBD.

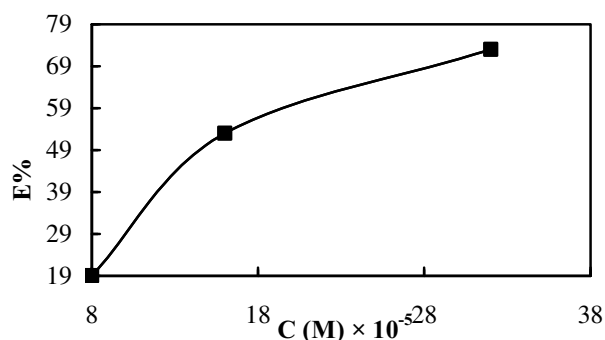


Fig. 3. Variation of the inhibition efficiency with different concentration of BAPD.

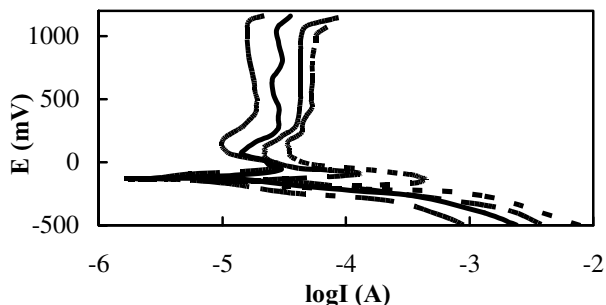


Fig. 4. Polarization curves of stainless steel 302 recorded in 0.5 M H₂SO₄ containing different concentration (---) blank, (— —) 20 ppm, (—) 40 ppm and (— · ·) 80 ppm) of BCBD at 20 ± 1 °C.

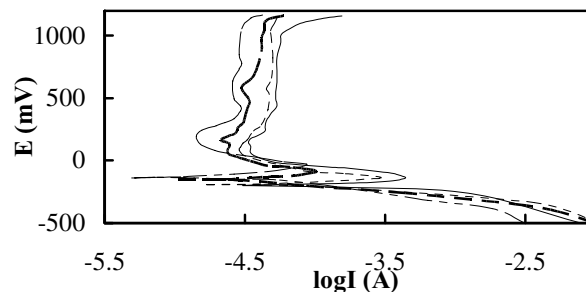


Fig. 5. Polarization curves of stainless steel 302 recorded in 0.5 M H₂SO₄ containing different concentration (---) blank, (— —) 20 ppm, (—) 40 ppm and (— · ·) 80 ppm of BAPD at 20 ± 1 °C.

measurements. Polarization curves for stainless steel in 0.5 M H₂SO₄ in the absence and presence of BCBD and BAPD at 20 ± 1 °C are shown in Figs. 4 and 5.

The electrochemical parameters for the alloy in acid solution derived from polarization curves are given in Table 1. This includes: corrosion potential (E_{corr}), corrosion current density (I_{corr}), critical current density (I_{cr}), inhibition efficiency (η) and surface coverage degree (θ). The percentage inhibition efficiency ($\eta\%$) and surface coverage (θ) are obtained from the following relations:

$$\eta\% = (I_0 - I/I_0) \times 100 \tag{3}$$

$$\theta = (I_0 - I/I_0) \tag{4}$$

where I_0 and I are the corrosion current densities obtained in the absence and presence of the inhibitor. The highest inhibition efficiency of 92.5% was found at a concentration of 16.2 M BCBD.

An inspection of the results obtained from Table 1 reveals that the increase in the concentration of the additive compounds indicates the following:

(i) Increase of both anodic and cathodic Tafel slopes indicates a mixed anodic and cathodic act on the corrosion mechanism [17] *i.e.* mixed inhibitor.

Table 1. Electrochemical Parameters of Stainless Steel 302 in 0.5 M H₂SO₄ with out and with Different Concentrations of BCBD and BAPD

Concentration (M) × 10 ⁻⁵	log I_{corr} (A cm ⁻²)	-E (mV)	log I_{cri} (A cm ⁻²)	I_{corr} (μA cm ⁻²)	I_{cri} (μA cm ⁻²)	θ	η (%)
BCBD							
0	-4.12	200	-3.48	75.8	331.1	0	0
4.1	-4.65	155	-4.00	22.3	100	0.70	70.5
8.1	-5.12	130	-4.68	7.58	20.8	0.90	90.0
16.2	-5.25	130	-4.64	4.36	22.9	0.92	92.5
BAPD							
0	-4.12	200	-3.48	75.8	331	0	0
8	-2.40	195	-3.68	63.0	208	0.16	16
16	-4.44	170	-4.12	36.0	75	0.52	52
32	-4.68	140	-4.12	20.8	75	0.72	72

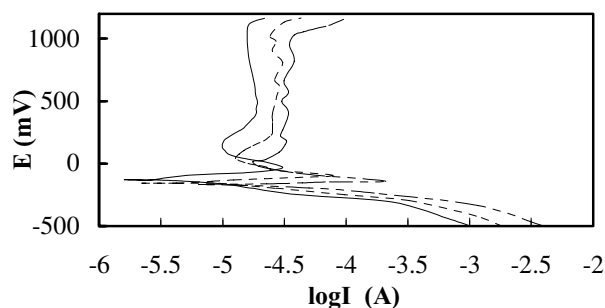


Fig. 6. Effect of temperature (—) 20 °C, (- - -) 30 °C and (- · - ·) 40 °C) on the cathodic and anodic responses for stainless Steel 302 in 0.5 M H₂SO₄ + 16 × 10⁻⁵ M of BCBD.

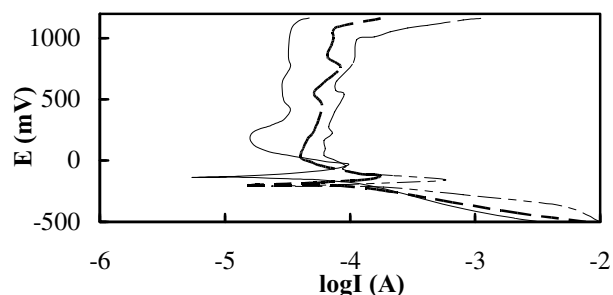


Fig. 7. Effect of temperature (—) 20 °C, (- - -) 30 °C and (- · - ·) 40 °C) on the cathodic and anodic responses for stainless Steel 302 in 0.5 M H₂SO₄ + 32 × 10⁻⁵ M of ADPA.

(ii) The IE calculated from weight loss and polarization measurements was found to increase with increasing the inhibitor concentration. Moreover, the inhibitor caused no change in the nature of anodic and cathodic Tafel slopes, indicating that it is first adsorbed onto iron surface and thus impedes the corrosion process by merely blocking the reaction sites of iron surface without affecting the anodic and cathodic reaction mechanism.

(iii) The current-density values decrease in the passive region as the concentration of inhibitors increases. The corrosion potential (E_{corr}) increases as the concentration of the inhibitor increases from 20 to 80 ppm. The corrosion current (I_{corr}) and critical current density (I_{cr}) decrease as the concentration of the inhibitors increases. Such a characteristic

behavior has been reported earlier [18-20].

Effect of Temperature

The temperature can modify the interaction between the stainless steel electrode and the acidic medium in the absence and the presence of the inhibitor [21].

Polarization curves for stainless steel in 0.5 M H₂SO₄ without and with 80 ppm of inhibitors in the temperature range 20-40 ± 1 °C are shown in Figs. 6 and 7 and the corresponding data are given in Table 2. The corrosion current density increases with increasing temperature in both uninhibited and inhibited solutions but the corrosion current density of steel increases more rapidly with temperature in the absence of the inhibitors.

Table 2. The Influence of Temperature on the Electrochemical Parameters for Stainless Steel 302 Electrode Immersed in 0.5 M H₂SO₄ Containing 16.2 × 10⁻⁵ M and 32 × 10⁻⁵ M of BCBD and BAPD Respectively

Temperature (±1 °C)	log I_{corr} (A cm ⁻²)	-E (mV)	log I_{cri} (A cm ⁻²)	I_{corr} (μA cm ⁻²)	I_{cri} (μA cm ⁻²)	θ	H (%)
BCBD							
20	-5.25	130	-4.64	4.3	22.9	0.92	92
30	-5.2	160	-4.2	6.3	63.0	0.91	91
40	-4.8	170	-3.8	15.8	158.4	0.80	80
BAPD							
20	-4.68	220	-4.12	2.08	7.5	0.72	72
30	-4.36	300	-3.84	4.36	1.44	0.42	42
40	-4.25	280	-3.36	6.3	4.36	0.16	16

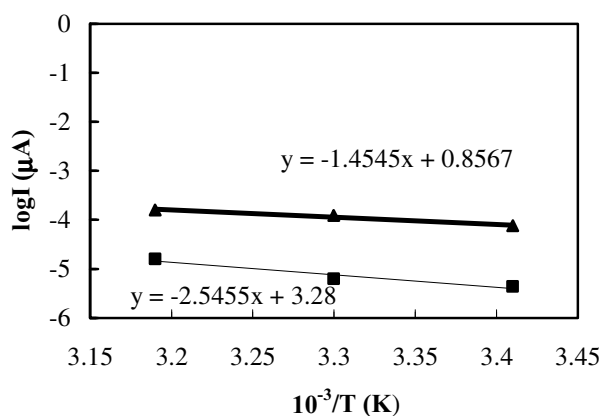


Fig. 8. Arrhenius slopes calculated from corrosion current density for stainless Steel 302 in: (▲) 0.5 M H₂SO₄ and (■) 0.5 M H₂SO₄ + 16 M of BCBD.

This proves that the inhibition occurs through the adsorption of the inhibitor on the metal surface [10].

Desorption was aided by an increase in temperature. The degree of coverage (θ) was found to increase with increasing the concentration of additive compounds and decreased as the temperature was raised from 20-40 ± 1 °C.

The activation energy of the corrosion process can be calculated using the following equation:

$$K = A \exp(-E_a/RT) \quad (5)$$

where E_a is the activation energy, A is the frequency factor, T is the absolute temperature, R is the gas constant and k is the rate of metal dissolution reaction which is directly related to corrosion current density (I_{corr}) [15]. Plotting k vs. 1/T, the value of E_a can be calculated from the slopes of straight lines (Figs. 8 and 9). The values of E_a obtained in 0.5 M sulfuric acid are listed in Table 3. The results agree with the order of

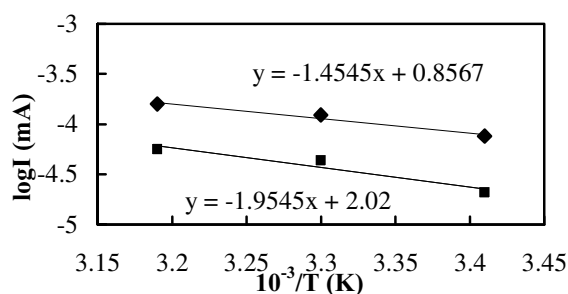


Fig. 9. Arrhenius slopes calculated from corrosion current density for stainless Steel 302 in: (◆) 0.5 M H₂SO₄ and (■) 0.5 M H₂SO₄ + 32 M of BAPD.

IE. The activation energy was higher in the presence of the inhibitor than in its absence. This type of the inhibitor retards the corrosion process at ordinary temperature [22-23], whereas the inhibition is considerably decreased at elevated temperatures.

Adsorption Isotherm

The nature of inhibitor interaction on the corroding surface during corrosion inhibition of metals and alloys has been deduced in terms of adsorption characteristics of the inhibitor [24-25].

The degree of surface coverage (θ) for different concentrations of inhibitors in the acid has been evaluated from polarization measurement values. The values of (θ) have been inserted into Tables 1 and 2. The degree of surface coverage was found to increase with increasing the concentration of additive compounds, and decreased as the temperature was raised from 20-40 ± 1 °C. The data were tested graphically by fitting it to various isotherms. A straight line was obtained on plotting C/ θ vs. C (Figs. 10 and 11) suggesting that the adsorption of the compounds from the acid

Table 3. Activation Energy (E_a) of Corrosion, Enthalpy and Free Gibbs Energies of Schiff Bases Adsorption Obtained from Polarization Measurements

Inhibitor	E_a (kJ mol ⁻¹)	ΔH (kJ mol ⁻¹)	ΔG (kJ mol ⁻¹)	ΔS (kJ mol ⁻¹ K ⁻¹)
Blank	27.8	-	-	-
BCBD	37.4	-53.0	-27.9	-0.08
BAPD	48.7	-43.4	-24.9	-0.06

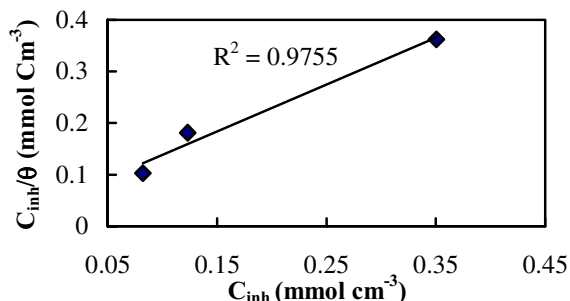


Fig. 10. Langmuir isotherm adsorption model on the steel surface of BCBD in 0.5 M H₂SO₄.

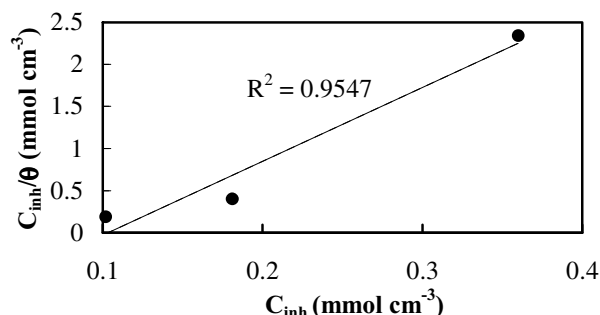


Fig. 11. Langmuir isotherm adsorption model on the steel surface of BAPD in 0.5 M H₂SO₄.

on stainless steel surface followed Langmuir adsorption isotherm.

The free energy of adsorption (ΔG_{ads}) at different temperatures was calculated from the following equations:

$$\Delta G_{\text{ads}} = -RT \ln(55.5K) \quad (6)$$

and K is given by:

$$K = \theta/C (1-\theta) \quad (7)$$

where θ is the degree of coverage on the metal surface, C is the concentration of inhibitor in M and K is the equilibrium constant. The value of ΔG_{ads} is given in Table 3. The low and negative values of ΔG_{ads} indicate the spontaneous adsorption of the inhibitor on the surface of SS302. The negative values of ΔG_{ads} are indicative of the strong interaction of the inhibitor molecules with the alloy surface [26-27].

The plot $\log(\theta/(1-\theta))$ vs. $\log C$ was found to be linear for this inhibitor (Fig. 12). The equilibrium constant (K) for adsorption-desorption process for this compound can be calculated from reciprocal antilogarithm of intercept.

The Langmuir adsorption isotherm [28] may be expressed by:

$$\theta/1 - \theta = AC \exp(-\Delta H/RT) \quad (8)$$

where T is temperature A is independent constant, C is inhibitor concentration, R is gas constant, ΔH is heat of adsorption and θ is surface coverage by the inhibitor molecule.

Eq. (3) can be converted to logarithmic scales:

$$\log(\theta/(1-\theta)) = \log A + \log C - \Delta H/2.303RT \quad (9)$$

Plot of $\log(\theta/(1-\theta))$ vs. $(1/T)$ at constant additive concentration is shown in Fig. 13. The slope of the linear parts of the curves is equal to $-\Delta H/2.303R$ from which the average heat of adsorption ΔH was calculated whose value is given in Table 3.

The negative values of ΔH reflect the exothermic behavior of inhibitors on the stainless steel surface. The differences in the inhibition efficiencies of the two compounds depend on their structures, since both of the molecules are attached to the surface of the alloy. The color and benzene rings groups on BCBD tend to increase the electron density on the C=N group, increasing the bond strength between the molecule and the metal surface under these circumstances. Therefore, the inhibition efficiency of BCBD should be higher than that of BAPD, as was observed.

CONCLUSIONS

BCBD and BAPD inhibit stainless steel corrosion in sulphuric acid solution. The inhibition efficiency increased with concentration but decreased with a rise in temperature. The inhibitor molecules were physically adsorbed on the metal surface following Langmuir adsorption isotherm. The thermodynamic values (E_a , ΔH , ΔG and ΔS) obtained show that the presence of the inhibitors increases the activation energy, while the negative values of ΔG indicate the

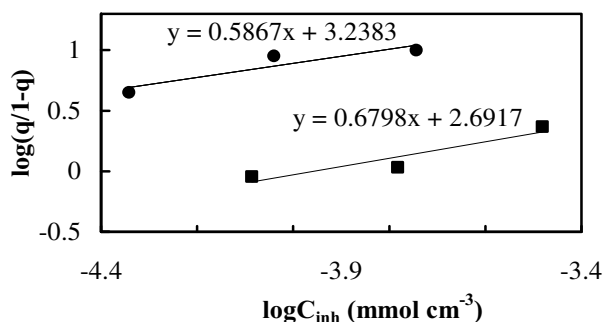


Fig. 12. Plot of $\log(\theta/1-\theta)$ vs. $\log C$ for stainless Steel 302 in 0.5 M H_2SO_4 solution at 20 ± 1 °C ((■) ADPA and (●) BCBD).

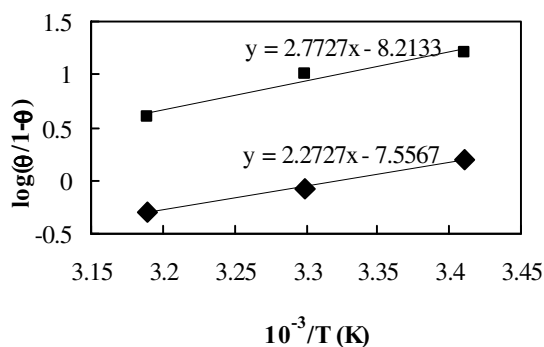


Fig. 13. Plot of $\log(\theta/1-\theta)$ vs. $1/T$ for mild steel in 0.5 M H_2SO_4 solution containing 16×10^{-5} M and 32×10^{-5} M of BCBD (■) and BAPD (◆) respectively.

spontaneous adsorption of the inhibitors on the surface of stainless steel.

REFERENCES

- [1] K.K. Al-Neami, A.K. Mohamed, I.M. Kenawy, A.S. Fouda, *Monatsh. Chem. (Chemical Monthly)* 126 (1995) 369.
- [2] M.T. Mokhalouf, A.S. El-Shahawy, S.A. El-Shatory, *Mater. Chem. Phys.* 43 (1996) 153.
- [3] M. Abdallah, H.E. Megahed, A.M. Atia, *J. Electrochem. Soc. India* 47 (1998) 35.
- [4] M.A. Quraishi, M.A. Wajidkhan, M. Ajmal, *Bull. Electrochem.* 11 (1995) 274.
- [5] S.S. Abd-El-Rehim, M.A. M.Ibrahim, K.F. Khaled, *J. Appl. Electrochem.* 29 (1999) 593.
- [6] P.R.P. Rodrigues, I.V. Aoki, A.H.P. Deandrade, E. Deoliveira, S.M.L. Agostinho, *Brit. Corros. J.* 31 (1996) 305.
- [7] A. Singh, R.S. Chaudhary, *Brit. Corros. J.* 31 (1996) 300.
- [8] S.M.A. Hosseini, M. Quanbari, M. Salari, *Indian J. Chem. Technol.* 14 (2007) 376.
- [9] A.El. Kanouni, S. Kertti, A. Srhiri, K. Bachir, *Bull. Electrochem.* 12 (1996) 517.
- [10] F. Zucchi, G. Tababelli, G. Brunoro, *Corros. Sci.* 33 (1992) 1135.
- [11] J. Uhrea, K. Armaki, *J. Electrochem. Soc.* 138 (1991) 2237.
- [12] S.M.A. Hosseini, S. Tajbakhsh, *Z. Phys. Chem.* 221 (2007) 1.
- [13] S.M.A. Hosseini, A. Azimi, *Mater. Corros.* 59 (2008) 41.
- [14] J.O.M. Bockris, B. Yang, *J. Electrochem. Soc.* 138 (1991) 2237.
- [15] G. Banerjee, S.N. Malhotra, *Corros.* 48 (1992) 10.
- [16] S.S. Abdel-rehim, M.A.M. Ibrhim, K.F. Khaled, *J. Appl. Electrochem.* 29 (1999) 593.
- [17] F. Hanna, G.M. Sherbini, Y. Barakat, *Brit. Corros. J.* 24 (1989) 269.
- [18] K. Bhrara, G. Singh, *Appl. Surf. Sci.* 253 (2006) 846.
- [19] V.K. Singh, V.B. Singh, *J. Mater. Sci.* 25 (1990) 690.
- [20] A. Bellaouchou, B. Kabkab, A. Guenbour, A. Ben, A. Bachir, *Prog. Org. Coat.* 41 (2001) 121.
- [21] M. Abdallah, *Corros. Sci.* 44 (2002) 717.
- [22] O.L. Riggs, R.M. Hurd, *Corrosion* 33 (1967) 252.
- [23] I.K. Putiolova, S.A. Balezin, Y.P. Barasanik, *Metallic Corrosion Inhibitors*, Pergamon Press, Oxford, 1960, p. 30.
- [24] R.K. Dinnapa, S.M. Mayanna, *J. Appl. Electrochem.* 11 (1982) 111.
- [25] R.K. Dinnappa, S.M. Mayanna, *Corros.* 38 (1982) 525.
- [26] M. Elachouri, M.S. Hajji, M. Salem, S. Kertit, J. Aride, R. Coudert, E. Essasi, *Corrosion* 52 (1996) 103.
- [27] B.V. Savithri, S. Mayanna, *Indian J. Chem. Technol.* 3 (1996) 2260.
- [28] M. Abdallah, *Corros. Sci.* 44 (2002) 717.